

The Structures Expected in a Simple Ternary Eutectic System:

Part II. The Al-Ag-Cu Ternary System

D. G. MCCARTNEY, R. M. JORDAN, AND J. D. HUNT

Ternary alloys of various compositions from the aluminum rich corner of the Al-Ag-Cu system were directionally solidified at several different growth rates ranging from $6.4 \times 10^{-1} \text{ mm} \cdot \text{s}^{-1}$ to $5.6 \times 10^{-3} \text{ mm} \cdot \text{s}^{-1}$. The region of two phase coupled growth between α -Al and CuAl_2 was determined at a growth rate of $6.4 \times 10^{-1} \text{ mm} \cdot \text{s}^{-1}$. The composition range over which a fully ternary eutectic structure formed was investigated for several different growth rates. The results are found to be consistent with the predictions of the competitive growth model set out in Part I,¹ and it would seem that the ternary eutectic composition of the published phase diagram may be incorrect. Scanning electron microscopy, using the backscattered electron signal, was used, together with optical microscopy, to study the microstructures formed. The ternary eutectic between α -Al, Ag_2Al , and CuAl_2 was found to be semiregular, and the unusual morphology of the two phase dendrites between α -Al and Ag_2Al is explained.

IN the previous paper, Part I,¹ the ideas developed to predict the ranges of structure in a two component system were extended, and used to predict the structural regions in a three component system. This paper sets forth the results of the experimental work on determining these structural regions in the Al-Ag-Cu ternary system in which a ternary eutectic had been observed² to form from α -Al, CuAl_2 and Ag_2Al .

EXPERIMENTAL PROCEDURE

The experimental apparatus for directionally solidifying specimens under a controlled temperature gradient and growth rate is shown schematically in Fig. 1. The specimens were contained in graphite crucibles 205 mm long, 6 mm OD and 4 mm ID, and directional solidification was achieved by withdrawing the graphite crucible at a constant rate from the hot zone of a wound resistance furnace into a water bath by means of a variable speed DC motor. The specimen could be quenched during growth by disengaging the motor drive and rapidly pulling the graphite crucible down into the water bath.

A standard technique was employed in making up alloys of the required composition, from pure aluminum (99.9 pct), copper (99.9 pct) and silver (99.9 pct), and casting them into the graphite crucibles. After filling, a graphite crucible was inserted into the growth furnace and allowed to equilibrate for up to 30 min under an argon atmosphere before directional solidification was begun. The growth rate during each run was monitored by noting the specimen position vs time and steady state

growth was continued for 50 mm before being terminated by rapid quenching into the water bath.

The temperature gradient was not measured for each run but several runs were made with a thermocouple in the specimen to obtain a measure of the gradient. A fine alumina sheathed chromel/alumel thermocouple was placed transversely across the specimen and its output was measured as a function of time during growth. From this it was found that the temperature gradient in the liquid at the interface was approximately $12^\circ\text{C}/\text{mm}$ in all specimens.

RESULTS

The approach to the investigation of the two and three phase coupled regions was based on the published phase diagram³ which is shown in Fig. 2. The ternary eutectic composition of Fig. 2, however, is not the composition which Cooksey and Hellawell² used to produce a fully ternary eutectic structure.

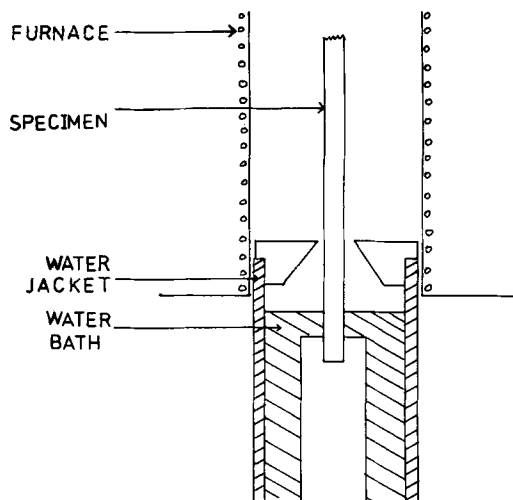


Fig. 1—Unidirectional growth apparatus.

D. G. MCCARTNEY, formerly with Alcan Laboratories Ltd., Banbury, Oxon, United Kingdom, is now Research Student, Department of Metallurgy and Science of Materials, Oxford University, Oxford, United Kingdom, R. M. JORDAN, formerly with Alcan Laboratories Ltd., is now with Alcan Canada Products, Arvida, Quebec, Canada, and J. D. HUNT is Lecturer, Department of Metallurgy and Science of Materials, Oxford University.

Manuscript submitted May 14, 1979.

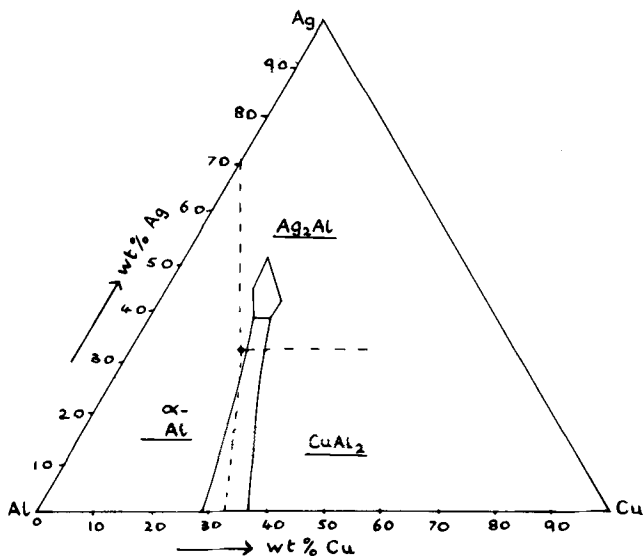


Fig. 2—Al-Ag-Cu phase diagram showing the eutectic valleys³ (dashed lines) and the boundaries of the two and three phase coupled growth regions (solid lines) determined in this work at a growth rate of 6.4×10^{-1} mm/s.

It was decided firstly to delineate the two phase coupled growth region between α -Al and CuAl_2 at constant growth rate and temperature gradient, then to locate the three phase coupled growth boundaries under the same conditions, and finally to determine how the shape of the three phase coupled region changes with growth rate. The results are thus divided into two groups as follows:

a. The Two Phase Coupled Growth Region between α -Al and CuAl_2 (θ)

The exact boundaries of this region were determined by directionally freezing a series of alloys with constant silver contents but whose copper contents varied by 1 wt pct Cu and spanned the eutectic valley. The constant silver levels were taken at regular intervals between 0 and 42 pct Ag and a growth rate of 6.4×10^{-1} mm·s⁻¹ was chosen in order to obtain a wide coupled region.

After solidification longitudinal and transverse sections of a specimen were mounted, examined using

optical and scanning electron microscopy, and classified as primary dendritic or fully eutectic. These classifications correspond to the schematic diagrams of Fig. 3 in Part I such that Figs. 3(d), (e), and (f) are primary dendritic, Fig. 3(b) is two phase dendritic and Figs. 3(a) and (c) are two and three phase eutectic respectively. The results are given in Table I and the two phase coupled region is plotted in Fig. 3 for the relevant portion of the phase diagram.

It was often difficult to resolve the fine two and three phase regions of the specimens and to distinguish between the phases using optical metallographic techniques. It was found, however, that scanning electron microscopy of specimens using the backscattered electron signal enabled the fine structures to be resolved with good contrast between the phases. Typical optical and backscattered electron micrographs are shown in Figs. 4(a) to (g) and the compositions to which they relate are shown on Fig. 3. Figures 4(a), (b), and (c)

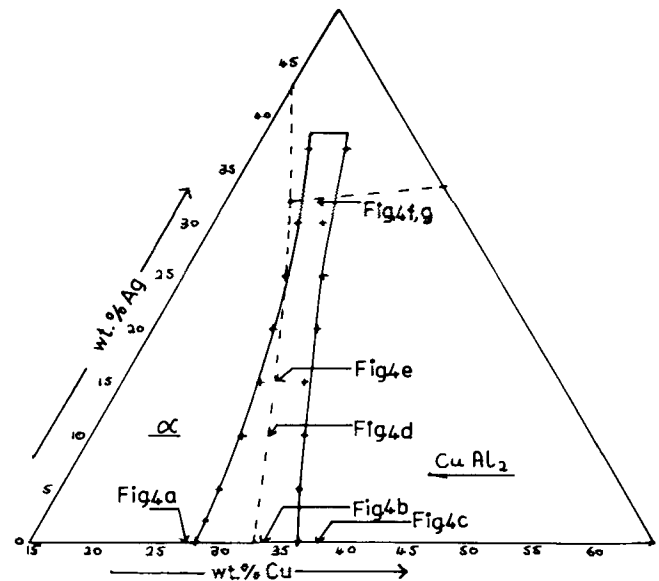


Fig. 3—Part of the published phase diagram³ showing the eutectic valleys (dashed lines) and the experimentally determined boundaries of the two phase ($\alpha + \theta$) coupled region (solid lines) at a growth rate of 6.4×10^{-1} mm/s. The arrows indicate the compositions of the specimens shown in Fig. 4.

Table I. Summary of the Experimental Results for Coupled Growth Between α -Al and CuAl_2

2 Pct Ag	5 Pct Ag	10 Pct Ag	15 Pct Ag	20 Pct Ag	25 Pct Ag	30 Pct Ag	37 Pct Ag	39.5 Pct Ag
Wt Pct	Wt Pct	Wt Pct	Wt Pct	Wt Pct	Wt Pct	Wt Pct	Wt Pct	Wt Pct
Cu Structure	Cu Structure	Cu Structure	Cu Structure	Cu Structure	Cu Structure	Cu Structure	Cu Structure	Cu Structure
28.2 α	27.2 α	26.5 α	25.5 α	24.0 α	22.5 α	21.0 α	18.5 α	18.0 α
29.2 $\alpha + \theta$	28.2 $\alpha + \theta$	27.5 $\alpha + \theta$	26.5 $\alpha + \theta$	25.0 $\alpha + \theta$	23.5 $\alpha + \theta$	22.0 $\alpha + \theta$	19.5 $\alpha + \theta$	19.0 $\alpha + \theta$
31.2 $\alpha + \theta$	32.3 $\alpha + \theta$	28.5 $\alpha + \theta$	29.0 $\alpha + \theta$	27.5 $\alpha + \theta$	24.5 $\alpha + \theta$	23.0 $\alpha + \theta$	21.5 $\alpha + \theta$	21.0 $\alpha + \theta$
32.2 $\alpha + \theta$	33.2 $\alpha + \theta$	31.5 $\alpha + \theta$	30.0 θ	28.5 θ	25.5 $\alpha + \theta$	24.0 θ	23.0 θ	22.0 θ
33.2 $\alpha + \theta$	34.2 θ	32.5 θ			26.5 θ			
34.2 $\alpha + \theta$								
35.2 $\alpha + \theta$								
36.2 θ								

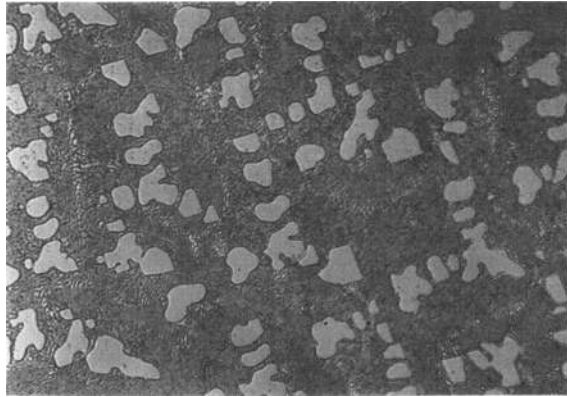
α = Primary α -Al dendrites present.
 θ = Primary CuAl_2 present.
 $\alpha + \theta$ = Two phase coupled growth.

show primary α -Al dendrites, two phase eutectic cells and primary CuAl_2 respectively in the nominally binary system. Figures 4(d) and (e) are longitudinal and transverse sections of two phase dendrites and the latter clearly shows that there are three phases present in the interdendritic material. Figure 4(f) shows the large volume fraction of ternary eutectic which forms around the two phase dendrites when the composition is close to the three phase coupled zone, and Fig. 4(g) is a

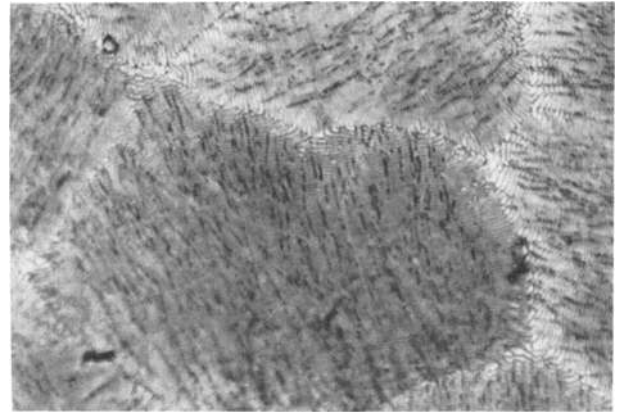
backscattered electron micrograph which clearly reveals the three phases present in the interdendritic regions.

b. The Three Phase Coupled Growth Region between α -Al, CuAl_2 and Ag_2Al

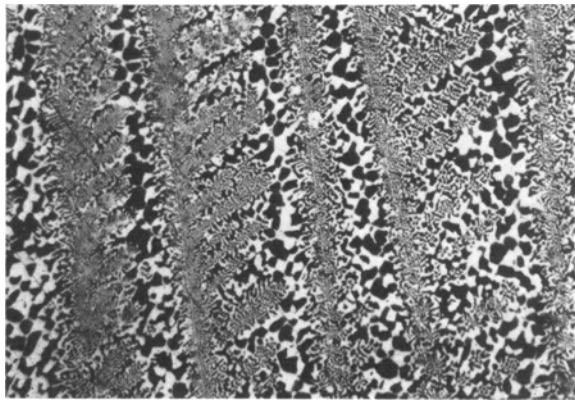
The composition range of three phase coupled growth was determined at three different growth rates namely 6.4×10^{-1} , 6.3×10^{-2} and $5.6 \times 10^{-3} \text{ mm/s}^{-1}$ with the



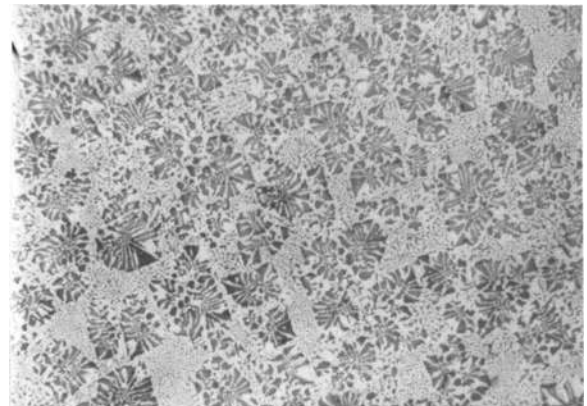
(a)



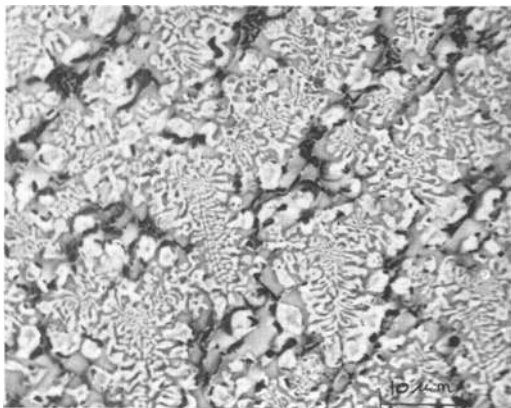
(b)



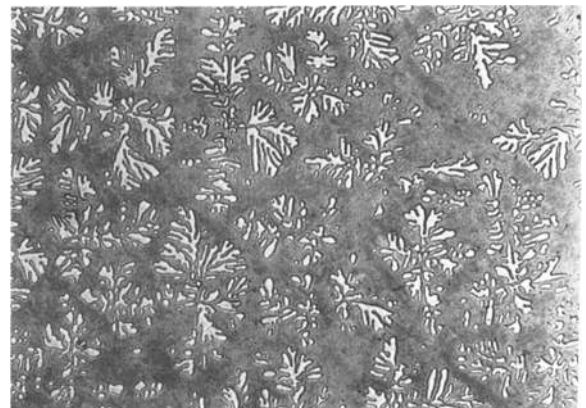
(c)



(d)

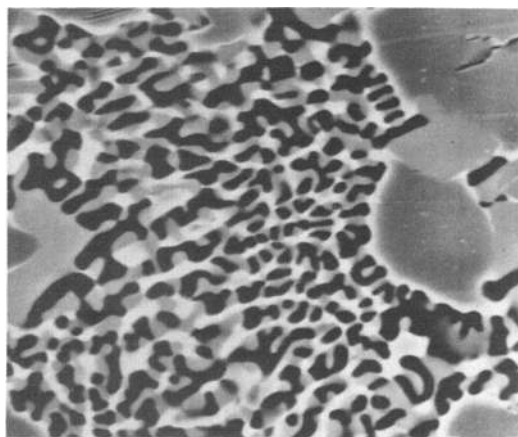


(e)



(f)

Fig. 4—(a) Transverse section showing primary dendrites of α -Al in a eutectic matrix. Optical micrograph, magnification 300 times, (b) transverse section through a specimen with a two phase eutectic microstructure. Optical micrograph, magnification 500 times, (c) transverse section showing primary CuAl_2 in a eutectic matrix. Optical micrograph, magnification 300 times, (d) longitudinal section showing two phase dendrites of α -Al and CuAl_2 , and coarse interdendritic material. Optical micrograph, magnification 300 times, (e) transverse section showing two phase dendrites of $(\alpha + \theta)$, with Ag_2Al (black) in interdendritic regions. Backscattered electron micrograph, magnification 500 times. (f) transverse section showing $(\alpha + \theta)$ dendrites in a ternary eutectic matrix. Optical micrograph, magnification 300 times, and (g) backscattered electron micrograph clearly showing the three phase nature of the interdendritic material, magnification 1500 times.



(g)

Fig. 4—Continued.

same temperature gradient as before. The boundaries of this coupled region were located by preparing several series of alloys of constant silver contents but whose copper contents varied by 1 wt pct Cu. The constant silver levels were taken at intervals of 1 or 2 wt pct Ag. After each specimen had been directionally frozen it was classified as described previously though in this region it was necessary to distinguish between the α -Al, CuAl_2 and Ag_2Al primary structures and also between the various combinations of phases in two phase dendrites.

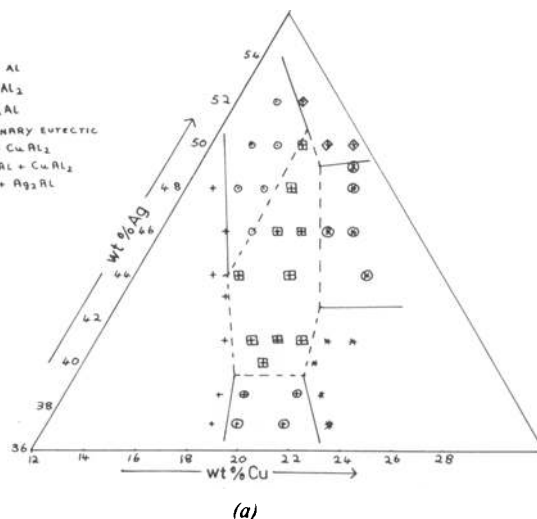
The graphs of Figs. 5(a) to (c) summarize the experimental information for the three different growth rates and are plotted for the relevant portion of the phase diagram. Figures 6(a) to (d) illustrate typical structures obtained at the highest growth rate. Figure 6(a) shows the ternary eutectic structure and Fig. 6(b) illustrates the two phase dendrites between CuAl_2 and Ag_2Al . The two phase dendrites between α -Al and Ag_2Al are shown in the transverse and longitudinal sections of Figs. 6(c) and (d).

DISCUSSION OF RESULTS

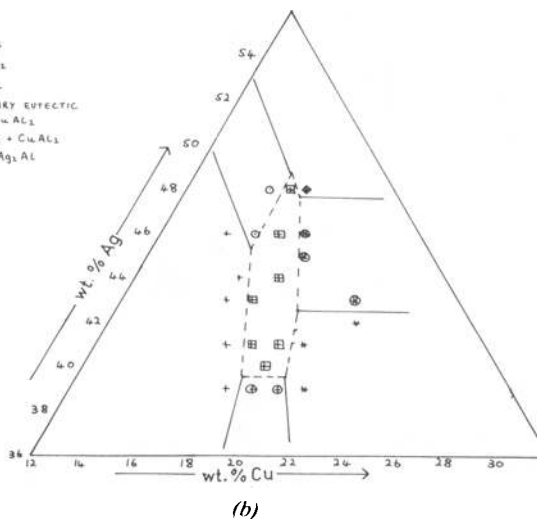
a. Characterization of Structural Regions

In the previous paper, Part I, it was predicted that five different structural regions are to be expected in a simple ternary eutectic system and the different structural regions and schematic growth interfaces predicted are shown in Figs. 2 and 3 of that paper. This work has confirmed the existence of several of these structural regions, and the types of solidified structures observed are in general consistent with the schematic growth interfaces which it was predicted would occur.

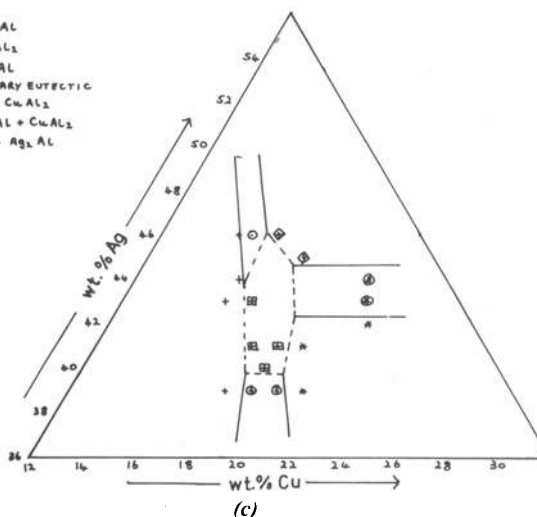
The results have shown that there is a region of three phase coupled growth, the shape of which is as predicted in Fig. 2 of Part I, and the composition range of which decreases with decreasing growth rate at the low values of G/V used which is also in agreement with the prediction of the competitive growth model used in Part I. This region of three phase coupled growth does not encompass the ternary eutectic composition of the phase diagram,³ but the composition of 41 pct Ag, 19 pct Cu at which Cooksey and Hellowell² located a



(a)



(b)



(c)

Fig. 5—(a) Relevant portion of the phase diagram showing the boundaries of the three phase coupled region (dashed lines) and two phase coupled regions (solid lines) at a growth rate of 6.4×10^{-1} mm/s, (b) relevant portion of the phase diagram showing the boundaries of the three phase coupled region (dashed lines), and two phase coupled regions (solid lines) at a growth rate of 6.3×10^{-2} mm/s, and (c) relevant portion of the phase diagram showing the boundaries of the three phase coupled region (dashed lines), and two phase coupled regions (solid lines) at a growth rate of 5.6×10^{-3} mm/s.

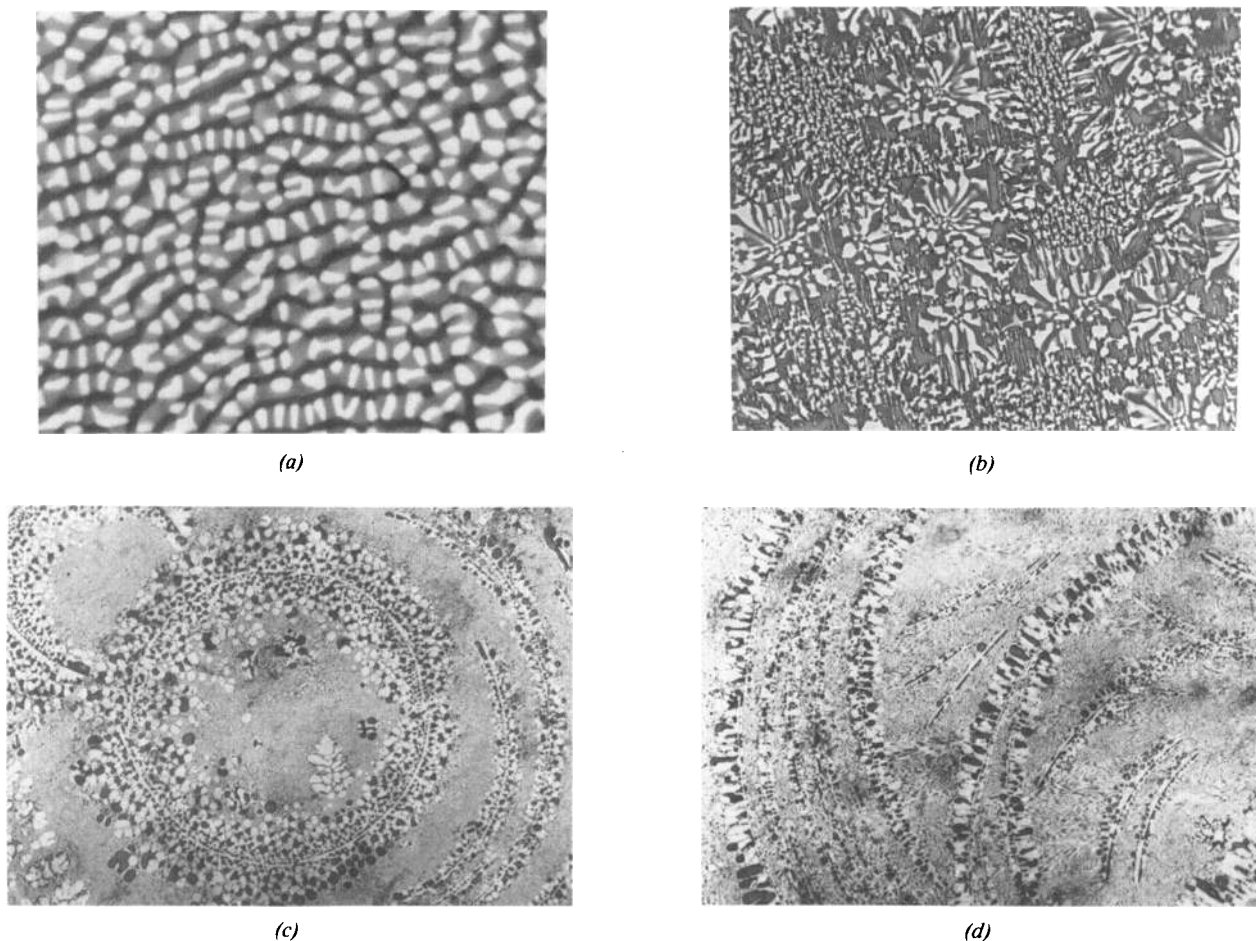


Fig. 6—(a) Transverse section showing the microstructure of a fully ternary eutectic specimen grown at 6.4×10^{-1} mm/s. α -Al is black, CuAl_2 grey and Ag_2Al white. Backscattered electron micrograph, magnification 5000 times, (b) transverse section showing two phase dendrites of CuAl_2 and Ag_2Al in a ternary eutectic matrix. Growth rate 6.4×10^{-1} mm/s. Backscattered electron micrograph, magnification 500 times, (c) optical micrograph showing two phase dendrites of α -Al and Ag_2Al in a ternary eutectic matrix. Growth rate 6.4×10^{-1} mm/s. Transverse section, magnification 300 times, and (d) optical micrograph showing two phase dendrites of α -Al and Ag_2Al in a ternary eutectic matrix. Growth rate 6.4×10^{-1} mm/s. Longitudinal section, magnification 300 times.

ternary eutectic structure lies well within this region and it would seem that this latter composition may be closer to the true ternary eutectic composition than that of the phase diagram. An important observation in this context is that the three phase coupled growth region shifts away from the ternary eutectic composition of the phase diagram at low growth rates. Three different two phase coupled regions have been located, as shown in Fig. 2, which run from the respective binary or pseudo-binary systems to the three phase coupled region as was predicted in Part I.

Two of the regions predicted—namely single phase planar front growth and two phase planar front growth—were not observed in this work. The reason for this is that these regions can be observed only at either very low impurity levels or very high values of G/V . The value of this parameter was approximately 20°C which was insufficient to maintain planar front eutectic growth even in the nominally binary Al-CuAl₂ eutectic as evidenced from Fig. 4(b).

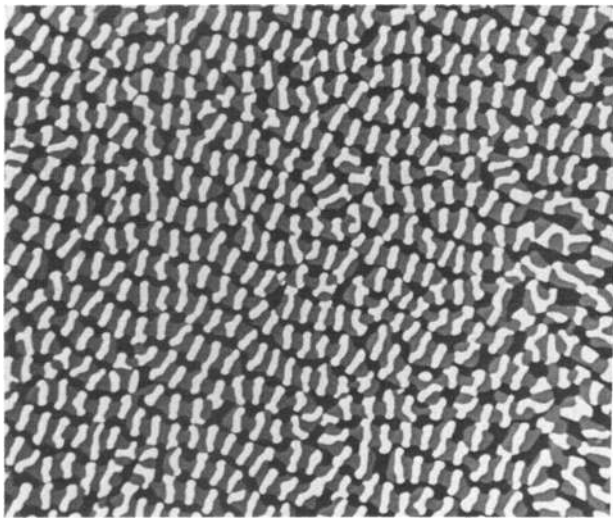
b. Microstructural Features

i. Ternary Eutectic. A transverse section of a fully ternary eutectic specimen solidified at 6.4×10^{-1} mm·s⁻¹ is shown in Fig. 6(a) while Figs. 7(a) and (b)

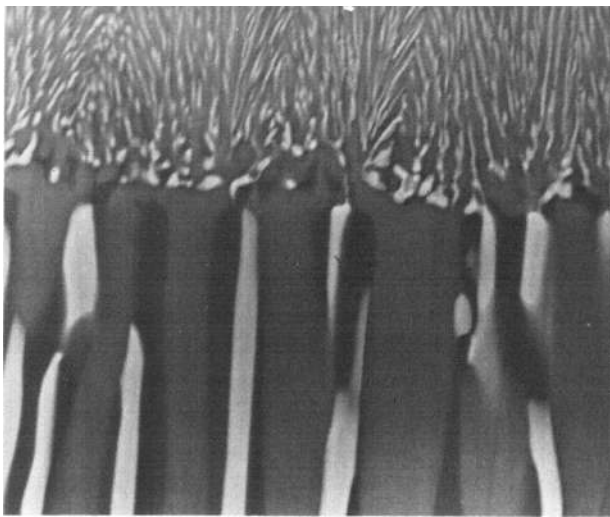
show a transverse section and a longitudinal section through the quenched interface of a specimen grown at 5.6×10^{-3} mm·s⁻¹. It is clear from the two transverse sections that the growth rate affects only the scale of the microstructure and from Fig. 7(b) it can be seen that the three phase eutectic freezes with a substantially planar, isothermal interface.

From the transverse sections of Figs. 6(a) and 7(a) it can be seen that the ternary eutectic structure is not completely irregular in that 'chains' of α -Al are separated from one another by 'chains' of CuAl_2 and Ag_2Al in which the two intermetallics form alternating 'links'. It is possible that this semiregular structure forms because the requirements of solute redistribution and the incompatibility of crystal structures prevent a completely regular growth morphology ever forming.

ii. Two Phase Dendrites between α -Al and Ag_2Al . The type of solid-liquid interface expected when the composition lies in the two phase coupled region is shown in Fig. 3(b) of Part I. However, the quenched interface structures of Figs. 8(a) and (b) together with Figs. 6(c) and (d) show that this type of idealized interface does not always occur, and that the morphology of the two phase dendrites changes with growth rate. At 5.6×10^{-3} cm·s⁻¹ [Fig. 8(a)] the two phase dendrites are straight but at the two higher growth rates bending is



(a)



(b)

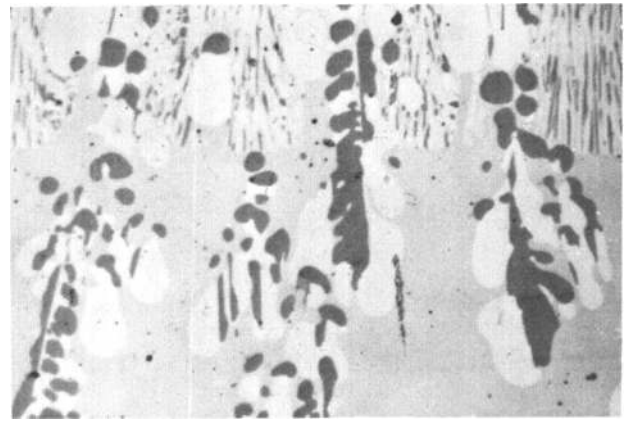
Fig. 7—(a) Backscattered electron micrograph showing a transverse section through a fully ternary eutectic specimen grown at 5.6×10^{-3} mm/s, magnification 600 times, and (b) backscattered electron micrograph showing a longitudinal section through the quenched interface of the specimen of Fig. 7(a), magnification 1800 times.

occurring at the growth interface. Clearly the two phase dendrites are in the form of thin sheets and these sheets are always bent with the α -Al phase on the inside of the curve. A possible explanation of this bending behavior is that the two phase sheets are behaving like bimetallic strips and are bending in the liquid ahead of the ternary eutectic interface. This will be possible since the sheets are growing in a temperature gradient and so there will be a temperature difference ΔT between the tip and the base as shown schematically in Fig. 9.

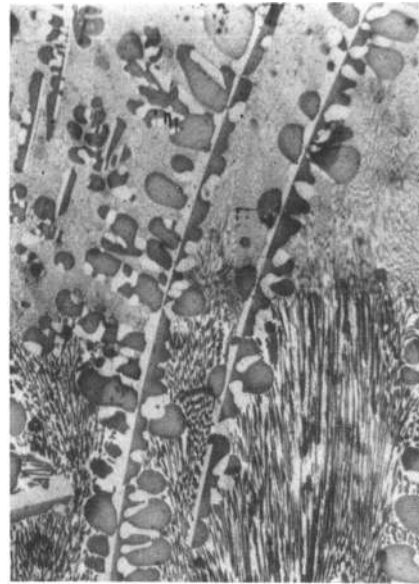
Assuming purely elastic behavior it can be shown that⁴ the curvature of a bimetallic strip is given by

$$\rho = \frac{1}{R} = \frac{3}{2} \cdot \frac{k_2 - k_1}{h} \cdot \Delta T$$

where ρ is the curvature, R the radius of curvature, k_1 and k_2 the coefficients of thermal expansion of the two phases ΔT is the temperature through which the strip is heated, and h is the thickness of the strip. In applying



(a)



(b)

Fig. 8—(a) Longitudinal section through the quenched interface showing two phase dendrites between α -Al (black) and Ag_2Al (white) for a growth rate of 5.6×10^{-3} mm/s, magnification 100 times, and (b) longitudinal section through the quenched interface showing two phase dendrites between α -Al (black), and Ag_2Al (white) for a growth rate of 6.3×10^{-2} mm/s, magnification 250 times.

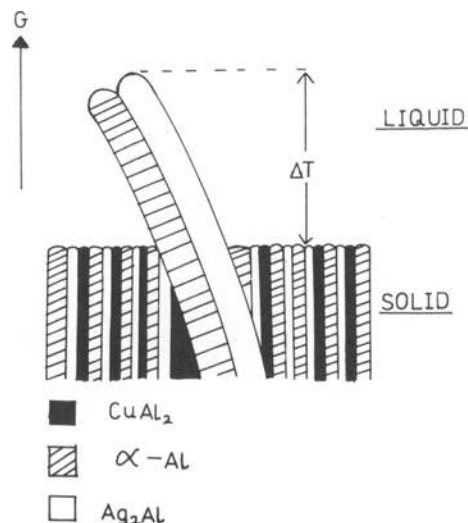


Fig. 9—Schematic representation of the growth interface when two phase dendrites of α -Al and Ag_2Al are present.

this model ΔT is taken as the temperature difference between the tip and base of the dendrite sheet. The coefficient of thermal expansion of Ag_2Al is unknown, but using the values for pure aluminum and CuAl_2 in Ref. 5 of $2.7 \times 10^{-5} \text{ K}^{-1}$ and $1.7 \times 10^{-5} \text{ K}^{-1}$ respectively then $(k_1 - k_2)$ will be of the order of 10^{-5} K^{-1} . The values of h for the different growth rates can be estimated from the micrographs and these are given in Table II together with the calculated radii of curvature.

From these results it is predicted that the curvature of the two phase dendrites is negligible at the lowest growth rate, and that it increases with increasing growth rate which is what is observed.

SUMMARY

i) Several of the structural regions of a simple ternary eutectic system which were predicted in Part I have been observed in this work, and it is assumed that it would be possible to locate the remaining regions under conditions of sufficiently high G/V or using sufficiently pure starting materials.

ii) The boundaries of the region of three-phase coupled growth are as predicted in Part I and it has been found that at the low values of G/V employed the range of three phase coupled growth decreases with decreasing growth rate which is consistent with the predictions of the competitive growth model used in Part I.

iii) The ternary eutectic was found to have a semi-regular structure, and the two phase dendrites between

Table II. Calculated Values of the Radii of Curvature (R) for Different Growth Rates Using Measured Thicknesses (h)

Growth rate, mm/s^{-1}	h , mm	R , mm
5.6×10^{-3}	10^{-1}	1.7×10^3
6.3×10^{-3}	6×10^{-3}	10^2
6.4×10^{-2}	1.7×10^{-3}	28

α -Al and Ag_2Al were found to be bent at the growth interface. This latter observation was explained by noting that these two phase dendrites, which are in the form of thin sheets, are growing in a temperature gradient and may be behaving like 'bimetallic strips'.

iv) The ternary eutectic composition of the published phase diagram seems to be incorrect and the composition 41 pct Ag, 19 pct Cu, is thought to be closer to the true value.

REFERENCES

1. D. G. McCartney, J. D. Hunt, and R. M. Jordan: *Met. Trans. A*, 1980, vol. 11A, p. 1243.
2. D. J. S. Cooksey and A. Hellawell: *J. Inst. Metals*, 1967, vol. 95, p. 183.
3. L. F. Mondolfo: *Aluminium Alloys—Structure and Properties*, pp. 420–21, Butterworths, London, 1976.
4. S. G. Starling and A. J. Woodall: *Physics*, pp. 151–53, Longmans, London, 1957.
5. I. G. Davies and A. Hellawell: *Phil. Mag.*, 1969, vol. 19, p. 1285.